Targeting the Nrf2 Signaling Pathway in the Retina With a Gene-Delivered Secretable and Cell-Penetrating Peptide

Cristhian J. Ildefonso,[1] Henrique Jaime,[2] Emily E. Brown,[3] Ryo L. Iwata,[1] Chulbul M. Ahmed,[1] Michael T. Massengill,[1] Manas R. Biswal,[1] Shannon E. Boye,[3] William W. Hauswirth,[3] John D. Ash,[3] Qiuhong Li,[3] and Alfred S. Lewin[1]

[1]Department of Molecular Genetics & Microbiology, University of Florida College of Medicine, Gainesville, Florida, United States
[2]Department of Biology, University of Florida College of Liberal Arts and Sciences, Gainesville, Florida, United States
[3]Department of Ophthalmology, University of Florida College of Medicine, Gainesville, Florida, United States

Correspondence: Alfred S. Lewin, Department of Molecular Genetics & Microbiology, University of Florida College of Medicine, 1200 Newell Drive, PO Box 100266, Gainesville, FL 32610-0266, USA; lewin@ufl.edu.

Submitted: July 15, 2015
Accepted: December 17, 2015

Citation: Ildefonso CJ, Jaime H, Brown EE, et al. Targeting the Nrf2 signaling pathway in the retina with a gene-delivered secretable and cell-penetrating peptide. *Invest Ophthalmol Vis Sci*. 2016;57:372–386. DOI:10.1167/iovs.15-17703

Purpose. Oxidative stress has been linked to several ocular diseases, initiating an inflammatory response that increases tissue injury. The Nrf2 transcription factor regulates expression of antioxidant genes and is tightly regulated by Kelch-Like ECH-Associated Protein 1 (Keap-1). We evaluate the antioxidant and anti-inflammatory properties of an adeno-associated virus (AAV) vector delivering an Nrf2-derived peptide that binds Keap-1.

Methods. The sequence of the Nrf2 peptide was fused to a cell-penetrating peptide (Tat-peptide) sequence (TatNrf2mer). The effects of lentiviral-delivered TatNrf2mer were studied in vitro. Transcript (quantitative [q] RT-PCR) and protein levels (ELISA and immunofluorescence) were quantified. Cell viability was measured by MTT and Cell Titer assays. The AAV vectors were packaged with the TatNrf2mer fused to secretable green fluorescent protein (GFP) under the control of the small chicken β actin promoter. The protective effects of this vector were evaluated in a model of RPE oxidative injury and in a mouse model of uveitis after intravitreal injection.

Results. Expression of TatNrf2mer peptide induced antioxidant gene expression, blocked IL-1β secretion, and protected cells from oxidative injury. In mice, TatNrf2mer expression partially protected photoreceptor function based on ERG responses and optical coherence tomography measurements in the sodium iodate ($NaIO_3$) model. Furthermore, sGFP-TatNrf2mer expression decreased IL-1β and IL-6 in the $NaIO_3$-treated mice, and resulted in a 54% decrease in the number of inflammatory cells in the vitreous body of the endotoxin-induced uveitis mouse model.

Conclusions. The intravitreally delivered AAV-TatNrf2mer has antioxidant and anti-inflammatory effects in widely-used models of ocular injury, suggesting it also could be useful in ocular diseases associated with oxidative stress and inflammasome activation.

Keywords: AAV, oxidative stress, inflammation, geographic atrophy, retina

Oxidative stress has been associated with neurodegenerative diseases ranging from amyotrophic lateral sclerosis (ALS) to stroke.[1,2] Within the retina, oxidative stress is an important driving force for the development of dry age-related macular degeneration (dry-AMD).[3–5] In age-related neurodegeneration, mitochondria are a major source of toxic oxygen radicals, though superoxide generated by nicotinamide adenine dinucleotide phosphate (NADPH) oxidase also is thought to contribute to neural injury and inflammation.[6] Superoxide generated by mitochondrial electron transport is responsible, directly or indirectly, for injurious modifications to proteins, lipids, and DNA.[7,8] These oxidized molecules not only lose their biological function but also serve as damage-associated molecular pattern (DAMP) signals. Damage-associated molecular pattern signals, such as the reactive aldehyde 4-hydroxynonenal, have been detected in the retina and RPE of patients affected with dry-AMD.[9] An oxidation product of docosahexanoic acid, carboxyethyl pyrrole (CEP) induces a dry-AMD–like phenotype when injected in mice.[10]

Human cells have overlapping defense systems to protect against reactive oxygen species (ROS).[11] These systems include small molecules, such as glutathione and α-tocopherol, and enzymes, such as superoxide dismutases and catalase. Nuclear factor (erythroid-derived 2)-like 2, or Nrf2, is a transcriptional coinducer of a set of genes with antioxidant and detoxifying properties.[12] In addition, Nrf2 recently has been shown to be a negative regulator of NADPH oxidase subunit NOX2 in neuronal glial co-cultures.[13] Nrf2 is tightly regulated by its repressor Kelch-Like ECH-Associated Protein 1 (Keap-1) which, upon binding to Nrf2, recruits ubiquitin ligases that target Nrf2 for proteosomal degradation. When increases in oxidative stress occur, sulfhydryl groups on Keap-1 are oxidized. This allows Nrf2 to be released, phosphorylated,[12] and translocated into the nucleus where it upregulates genes under the control of the antioxidant response element (ARE).[14] These genes encode proteins that are responsible for the removal of noxious ROS and reactive nitrogen species (RNS).

In recent years, modulators of the Nrf2 signaling pathway have been of significant interest as potential therapeutic agents.

Investigative Ophthalmology & Visual Science

Studies in animal models of acute liver failure have suggested that the siRNA-mediated knockdown of Keap-1 could alleviate disease-associated pathology.[15] Other groups have studied the control of this signaling pathway by small molecules, such as the phytochemical sulforaphane, which modifies sufhydryls in Keap 1 and is protective in animal models of a several diseases.[16–18] Within the retina, the Nrf2 signaling pathway has shown to be a promising therapeutic target. Recently, Xiong et al.[19] demonstrated that delivery of *NRF2* cDNA protected photoreceptors and retinal ganglion cells from oxidative stress. An impaired Nrf2 signaling pathway has been implicated in the development of the RPE damage seen in AMD.[20] Interestingly, this same pathway seems to be of importance in the pathophysiology of ocular inflammatory diseases, such as uveitis. Nagai et al.[21] demonstrated that Nrf2 protected the retina from inflammation in a mouse model of uveitis. Taken together, these results suggest that stimulating the Nrf2 signaling pathway could have broad therapeutic benefit.

One approach to modulating the NRF2 signaling pathway is through the use of small peptides that bind Keap-1 and lead to the liberation of the Nrf2. Using a phage display library to screen for peptides that stimulate the ARE response, Hancock et al.[22] identified such peptides derived from p62, prothymosin-α and other proteins. In 2012, Steel et al.[23] showed that an Nrf2-derived peptide could activate downstream heme oxygenase 1 (*HO-1*) gene expression and inhibit TNF-α production in vitro. Although this peptide holds potential for therapy, it would require repeated administration to treat chronic inflammatory disease, such as AMD. Because of its demonstrated record of safety in treating ocular disease,[24–26] we asked whether adeno-associated virus (AAV)–mediated delivery of an Nrf2 peptide could alleviate oxidative stress in the retina. We described an AAV vector that delivers a secreted and cell-penetrating peptide derived from the Nrf2 protein, which allows the nuclear translocation of endogenous Nrf2 and the induction of *ARE* genes in vitro and in vivo. We also demonstrated that this vector can block secretion of proinflammatory cytokine IL-1β in cell culture while decreasing the recruitment of inflammatory cells to the vitreous in an animal model of uveitis.

Materials and Methods

Cell Culture

Human cell lines were grown at 37°C in the presence of 5% CO_2. The HEK293T cells were maintained in Dulbecco's modified Eagle's medium (DMEM), while ARPE-19 cells were grown in a 1:1 mixture of DMEM and F-12 medium (DMEM/F12, 50/50). All media were supplemented with fetal bovine serum (FBS) to a final concentration of 10% and with penicillin-streptomycin in a 1% final concentration. Media were filtered sterilized using a 0.22-μm filter unit. ARPE19 cells were validated by ATCC (Manassas, VA, USA) and were frozen immediately upon receipt. Only low passage cells were used in these experiments.

Design and Cloning the TatNrf2mer Sequence Into the pCDH-EF1-MCS-T2A-puroR Lentiviral Vector Plasmid

The Nrf2 amino acid sequence that interacts with Keap-1 protein is reported to be the following: LQLDEETGEFLPIQ. This sequence was fused downstream of the HIV Tat-peptide sequence (RKKRRQRRR) to generate the Nrf2 peptide (Nrf2mer) with cell-penetration properties. The complete amino acid sequence of the *TatNrf2mer* gene is as follows: RKKRRQRRRLQLDEETGEFLPIQ. Codons were selected and optimized for expression in mammalian cells using the J-Cat software.[27] Partially overlapping oligonucleotides were synthesized (Table 1). The uppercase and underlined sequence of these oligonucleotides represent complementary sequences with a melting temperature (T_M) of 65°C, while the uppercase and bold sequence represents the EcoRI (1) and NotI (2) restriction sites. Oligonucleotides were mixed, and single stranded sequences were filled-in using the Klenow fragment of *Escherichia coli* DNA polymerase I. Each reaction mixture contained 5 μg each oligo, 2 μL NEB buffer 2 (10×), 1 μL dNTPs mix (10 mM each), and 6 μL deionized H_2O. Hybridization of the oligonucleotides was achieved using the following conditions: Three cycles of 94°C for 30 seconds and 60°C for 30 seconds. The reaction was cooled to 15°C and 1 μL Klenow fragment (5 U/μL) was added to the reaction and incubated at room temperature for 15 minutes. The reaction was stopped by adding 1 μL 210 mM EDTA and incubating at 72°C for 20 minutes. This product was purified with the GenElute PCR clean-up kit (Sigma-Aldrich Corp., St. Louis, MO, USA). The purified fragment and the pCDH-EF1-MCS-T2A-puroR plasmid (Systems Biosciences, Mountain View, CA, USA) were digested with EcoRI and NotI for 2 hours at 37°C, and purified with the GelElute kit. The digested products were ligated using the T4 DNA ligase (New England Biolabs, Ipswich, MA, USA) by incubating at room temperature for 2 hours. Ligation plasmids were used to transform *E. coli* strain DH5α cells (Invitrogen, Grand Island, NY, USA), and transformed colonies were selected on LB plates containing ampicillin (100 μg/ mL).

Lentiviral and AAV Vector Production

Lentiviral vectors (LV) were generated with the pCDH-EF1α-MCS-T2A-Puro plasmid from System Biosciences (Mountain View, CA, USA) as we described previously.[28] Transgenes were sequenced by the di-deoxynucleotide method.[29]

The AAV vectors were constructed by inserting the TatNrf2mer coding sequence downstream of an *Ig_K-EGFP* gene, linked via furin cleavage site. Expression was driven by the CMV enhancer and the chicken β actin promoter (CBA promoter) (see Fig. 4). The entire insert was placed between inverted terminal repeat (ITRs) of the AAV2 present in the plasmid. This plasmid was propagated amplified in Sure 2 cells (Agilent Technologies, Santa Clara, CA, USA) and DNA was prepared by CsCl purification of DNA before packaging. Finally, AAV2(quad Y-F+T-V) viral particles were generated, purified, and titrated by the Vector Core of the Vision Center at the University of Florida (Gainesville, FL, USA).[30] This mutant variation of AAV2 has been shown to transduce many cell types within the retina after an intravitreal injection.[31]

Enzyme Linked Immunosorbent Assay (ELISA)

The concentration of IL-1β in the conditioned media of cell cultures was measured using a Human IL-1β ELISA kit purchased from RayBiotech (Norcross, GA, USA). A total of 100 μL media was assayed. Each biological replicate was evaluated in triplicates according to the manufacturers' instructions. The concentration of murine IL-1β, IL-6, and MCP-1 was determined with ELISA kits from Peprotech (Rocky Hill, NJ, USA) according to the manufacturer's protocol. All ELISA kits and antibodies used are listed on Table 2.

Immunofluorescence

Cells were grown in an 8-well chamber slide at 2×10^5 cells per chamber for 24 hours. Afterwards, cells were washed once with PBS (pH 7.4) and incubated with 2% paraformaldehyde in

Investigative Ophthalmology & Visual Science

Table 1. Sequences of Oligonucleotides Used

Name	Sequence (5′->3′)	Target Species
TatNrf2mer-F	tatGAATTCgccaccatgagg aagaagaggaggcagagGAG GAGGCTGCAGCTGGACGAG	Human
TatNrf2mer-R	ataGCGGCCGCctggatgggc aggaactcgccggtctcCTC GTCCAGCTGCAGCCTCCTC	Human
Tat-F	AGTTCTTGCAGCTCGGTG	Human
Puro-R	TCGCCACCATGAGGAAG	Human
NqO1-F	AAAGGACCCTTCCGGAGTAA	Human
NqO1-R	CCATCCTTCCAGGATTTGAA	Human
GSTM1-F	CTACCTTGCCCGAAAGCAC	Human
GSTM1-R	ATGTCTGCACGGATCCTCTC	Human
GAPDH-F	ACAGTCCATGCCATCACTGCC	Human
GAPDH-R	GCCTGCTTCACCACCTTCTTG	Human
β actin-F	AGCGAGCATCCCCCAAAGTT	Human
β actin-R	GGGCACGAAGGCTCATCATT	Human
HO-1-F	AGCCCCACCAAGTTCAAACA	Mouse
HO-1-R	GCAGTATCTTGCACCAGGCT	Mouse
NqO1-F	CGACAACGGTCCTTTCCAGA	Mouse
NqO1-R	CCAGACGGTTTCCAGACGTT	Mouse
GSTM1-F	GGGATACTGGAACGTCCGC	Mouse
GSTM1-R	GCTCTGGGTGATCTTGTGTGA	Mouse
Catalase-F	CGCAATCCTACACCATGTCG	Mouse
Catalase-R	AGTATCCAAAAGCACCTGCTCC	Mouse
β actin-F	CGAGCACAGCTTCTTTGCA	Mouse
β actin-R	TTCCCACCATCACACCCTGG	Mouse

Tat, trans-activator of transcription from HIV-1; *Puro-R*, puromycin resistance gene; *NqO1*, NAD(P)H dehydrogenase quinone 1; *HO-1*, heme oxygenase 1; *GSTM1*, glutathione S-transferase mu 1; *GAPDH*, glyceraldehyde 3-phosphate dehydrogenase.

PBS for 15 minutes at room temperature. Cells were washed three times with PBS and then incubated in PBS with 0.1% Triton X-100 (PBS-T) for 10 minutes at room temperature. Cells then were washed three times as done previously. Cells were blocked by incubating with 1% BSA, 1% goat serum in PBS with 0.1% Tween-20, and 0.3 M glycine for 1 hour. The anti-Nrf2 antibody was diluted to 1 μg/mL in PBS-T with 1% BSA and incubated with the cells for 1 hour at room temperature in a humidified chamber. Cells were washed as in previous steps and then incubated with an anti-rabbit antibody conjugated to Cy3 chromophore (1:500 dilution) and 4′,6-diamidino-2-phenylendole (DAPI; 1:1000 dilution) diluted in PBS-T with 1% BSA for 1 hour at room temperature in the dark. Cells then were washed as in the previous step and mounted using Fluoromount-G (Southern Biotechnology Associates, Inc., Birmingham, AL, USA). Pictures were taken using a fluorescence microscope.

Transfection

HEK293T cells were plated at 80% confluency in a 6-well plate. Plasmid DNA complexes were made by diluting 1 μg plasmid DNA and 2.5 μg linear polyethyleneimine[32] (PEI) in 100 μL PBS and incubated at room temperature for 5 minutes. Complexes were made by adding the diluted PEI to the diluted plasmid DNA and incubating for another 20 minutes at room temperature. The medium in each well was replaced with 2 mL serum and antibiotic-free medium before adding the complexes. Cells were incubated in the presence of the complexes for 18 hours (37°C, 5% CO_2) before medium was replaced with 3 mL fresh medium containing 10% FBS and 1% Pen-Strep. Cells were collected 24 hours later by trypsin digestion.

RNA Isolation

Total RNA was isolated from cell cultures using the RNeasy mini kit (QIAGEN, Valencia, CA, USA) according to the manufacturers' protocol. RNA was quantified by 260 nm absorbance and quality was verified by running an aliquot in a 1% agarose gel.

cDNA Synthesis

Complementary DNA was synthesized with the iScript cDNA synthesis kit (Bio-Rad, Hercules CA, USA). Briefly, 1 ng total RNA (10 μL) was mixed with 4 μL 5× iScript reaction mix, 5 μL RNAse free water, and 1 μL iScript reverse transcriptase. The following temperatures and times were used in the synthesis of the cDNA: 25°C for 5 minutes, 42° for 30 minutes, and 85°C for 5 minutes. cDNA was stored at −20°C until needed.

PCR for the Detection of TatNrf2mer Expression

A PCR reaction was prepared using 1 μL cDNA isolated from ARPE-19 cells or ARPE-19 cells expressing either puromycin resistance (*PuroR*) gene only (control) or TatNrf2mer. Primers binding the Tat region (Tat-F) and the PuroR region (PuroR-R) were used to detect TatNrf2mer mRNA (Table 1). Polymerase chain reaction conditions were as follows: 93°C for 3 minutes, 30 cycles of 93°C for 30 seconds, 55°C for 30 seconds, and 72°C for 20 seconds, followed by 72°C for 10 minutes.

Table 2. Antibodies and ELISA Kits

Reagent	Company	Catalog Number
Anti-Nrf2 antibody	Abcam (Cambridge, MA, USA)	ab31163
Anti-Nrf2 [EP1808Y] antibody	Abcam	ab62352
Anti-Lamin A+C [EPR4100] antibody	Abcam	ab108595
Goat anti-rabbit IgG (H+L) secondary antibody, Alexa Fluor 488 conjugate	Invitrogen	A-11034
Anti-GFP antibody, rabbit IgG fraction	Invitrogen	A11122
Nitrotyrosine ELISA Kit	Abcam	ab113848
Anti-ZO-1 antibody	Invitrogen	40-2200
Murine IL-1B Mini ELISA ABTS Development kit	Peprotech	900-M47
Murine IL-6 Mini ELISA ABTS Development kit	Peprotech	900-M50
Murine JE/MCP-1 Mini ELISA ABTS Development kit	Peprotech	900-M126
Human IL-1 beta ELISA	RayBiotech	ELH-IL1b

Investigative Ophthalmology & Visual Science

Polymerase chain reaction products were separated in a 1.3% agarose gel.

Real-Time PCR (RT-PCR) for ARE Genes

Real-time PCR for glutathione S-transferase mu 1 (*GSTM1*) and NAD(P)H dehydrogenase quinone 1 (*NqO1*) was performed using the SsoFast EvaGreen Supermix kit (Bio-Rad). Primer sequences are listed in Table 1.

PCR reaction mixtures contained 1 μL 1:10 dilution of cDNA library, 1 μL forward (F) primer (5 μM) and 1 μL reverse (R) primer (5 μM), 5 μL 2× SsoFast EvaGreen supermix, and 2 μL dH_2O. Simultaneous amplification of all genes was done using the following conditions: 95°C for 3 minutes, followed by 40 cycles of 95°C for 10 seconds, and 60°C for 20 seconds. Fluorescence was measured at the end of each cycle by using the Bio-Rad CFX96 thermocycler. Fold changes in gene expression were determined by the $^{\Delta\Delta}C_t$ method.[33]

MTT Assay

Cells were plated in a 96-well plate at 8×10^4 cells per well in 100 μL complete growth medium and incubated overnight at 37°C. The next day, medium was removed, cells were washed with PBS, then exposed to 200 μL serum- and antibiotic-free medium containing 800 μM H_2O_2. Cells then were incubated at 37°C for 6 hours, washed with PBS, and incubated with 200 μL MTT (tetrazolium) solution diluted in RPMI-1640 (500 μg/mL) at 37°C for 4 hours. Three wells without cells but containing 200 μL MTT were included in the plate. After 4 hours, the MTT solution was removed, and cells were incubated in 200 μL PBS for 15 minutes at room temperature. The absorbance at 570 nm was determined using a Varian Carry 50 plate reader (Palo Alto, CA, USA).

Cell Titer Assay

Cells were plated in a 96-well plate at 70% confluency. The following day, cells were placed in serum-free media containing paraquat (Sigma-Aldrich Corp.) at the concentration indicated and incubated for 48 hr. CellTiter Aqueous reagent (Promega, Madison, WI, USA) was added and cells were incubated for an additional 30 minutes. Absorbance at 490 nm was measured with a plate reader. Cell survival was calculated by subtracting the absorbance in untreated cells as 100%.

Endotoxin-Induced Uveitis (EIU) Mouse Model

All mice in this study were treated by procedures approved by the University of Florida Institutional Animal Care and Use Committee and in accordance with the ARVO Statement for the Use of Animals in Ophthalmic and Visual Research. One-month-old C57BL/6J mice were injected intravitreally with 1 μL sterile saline containing 3×10^9 vector genomes of AAV vector delivering either green fluorescent protein (GFP; left eye) or sGFP-TatNrf2mer (right eye). One month after injection, GFP expression was observed by fluorescence funduscopy using a Micron III fundus microscope and fluorescein filters. Uveitis was induced by intravitreal injection of LPS (25 ng/eye) and the number of infiltrative cells in histologic sections was quantified as described previously by our lab.[34]

Sodium Iodate ($NaIO_3$) Mouse Model of RPE Damage

One-month-old C57BL/6J mice were injected intravitreally with 3×10^9 vector genomes of AAV2 (quad Y-F+T-V) vector delivering either GFP (left eye) or sGFP-TatNrf2mer (right eye). One month later, mice were evaluated for expression of GFP using fluorescent funduscopy. One week later, mice were injected intraperitoneally with 35 or 25 mg/kg $NaIO_3$. After 7 days, retinal function was evaluated by full field scotopic electroretinogram (ERG) using the Espion Ganzfeld Profile system (Diagnosys UK Ltd., Cambridge, UK).

Electroretinogram (ERG)

Scotopic ERG analysis was used to measure the loss of rod function as previously published.[35,36] Mice were dark adapted overnight. The following day the mice were dilated with ocular drops of 1% atropine and 10% phenylephrine solutions. Mice then were anesthetized using a mixture of ketamine (20 mg/mL) and xylazine (0.8 mg/mL) in normal saline. Gold wire electrodes were placed over the corneas of anesthetized mice, the reference electrode was placed in the mouth, and grounding needle electrode was placed in the tail. Mice were stimulated with 2.7 cd.s/m^2 flashes of light and light stimulated voltage changes were recorded as a function of time. The value of the a-wave was measured from 0 μV reference to the peak of the initial negative deflection, and the b-wave was measured from the absolute peak of the a-wave to the peak of the positively deflection within 2000 ms of the flash stimulus. The much slower c-wave was measured from the baseline to the peak of the positive deflection that occurs between 1 to 4 seconds of the light flash.

Fundoscopy and Spectral-Domain Optical Coherence Tomography (SD-OCT)

Fundus images were taken using a Micron III retinal imaging microscope (Phoenix Research Laboratories, Pleasanton, CA, USA). For SD-OCT, we used a high resolution instrument from Bioptigen (Morrisville, NC, USA). The animals were positioned upright and the retina was imaged with the digital fundus camera or the SD-OCT instrument. In both cases, the objective lens (funduscope) or optical probe (OCT) was mobile and was positioned near the surface of the eye. Mice were anesthetized with ketamine and xylazine and their eyes dilated[28] before images were made. Segmentation analysis of the retina was performed using system software (Driver 2.0) from Bioptigen.

Flat Mount Immunofluorescence

Flat mounts were prepared as described previously.[37] Briefly, eyes were enucleated and washed in PBS followed by a fixation in 4% PFA-PBS for 10 minutes. Afterwards, an incision was made through the sclera with an 18-gauge (G) needle followed by another 20 minutes incubation in 4% PFA-PBS. Eyes were washed with PBS and the cornea, iris, lens, and neuroretina were removed surgically leaving the RPE/choroid attached to the eye cup. This was then sectioned into quadrants and flattened on a glass slide to stain as described in the immunofluorescence section.

Statistical Analysis

Values are reported as the average and error bars represent the standard error of the mean (SEM). For comparison of two groups, Student's *t*-test for paired samples was performed. When more than two groups were compared, an ANOVA test was conducted followed by a student Newman-Keuls test to identify the differences between each group. Statistical significance was defined by a P value of ≤ 0.05. Data were analyzed using GraphPad Prism 5 software (La Jolla, CA, USA); $^*P \leq 0.05$, $^{**}P \leq 0.01$, $^{***}P \leq 0.001$.

Investigative Ophthalmology & Visual Science

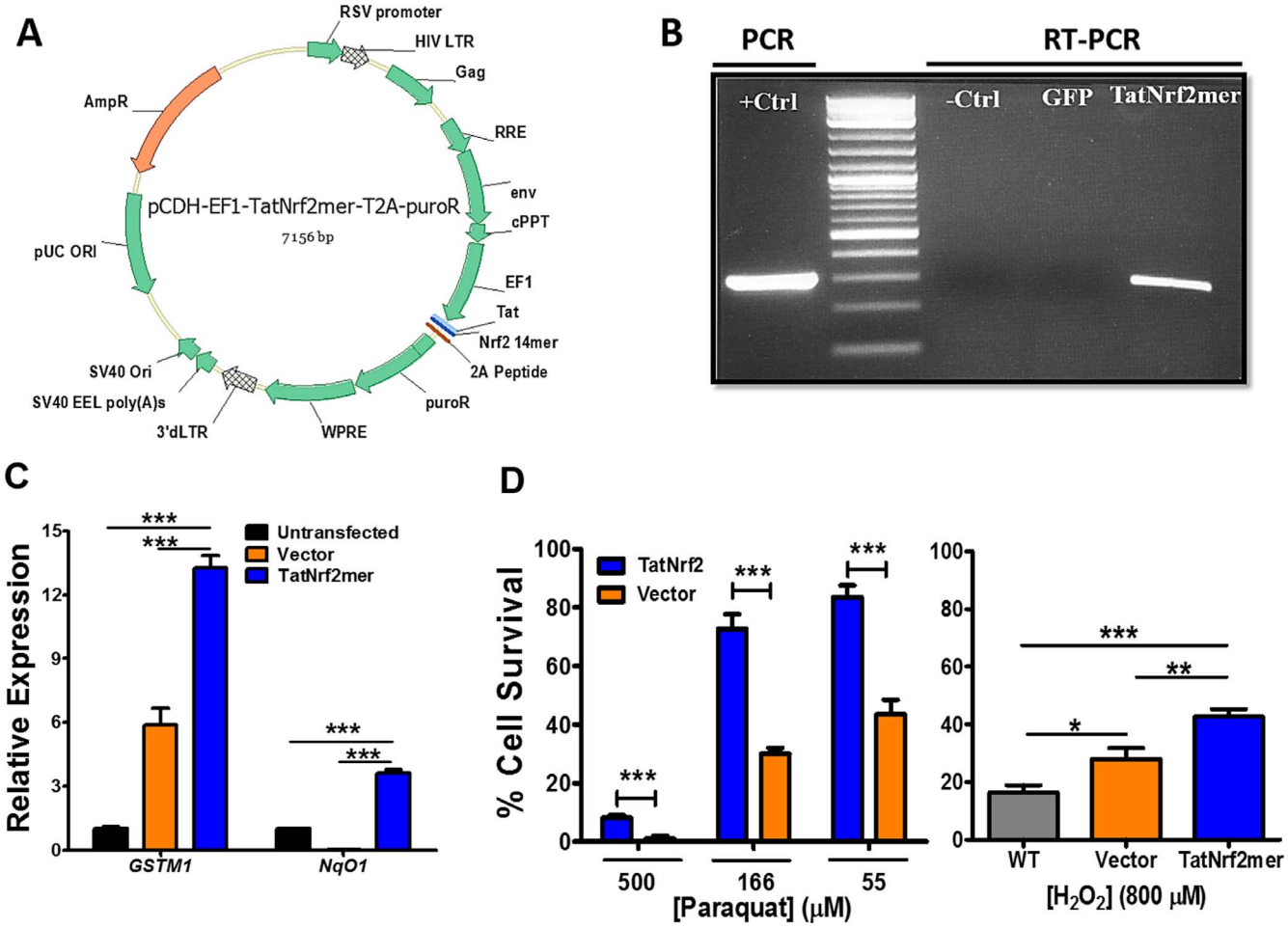

Figure 1. The TatNrf2mer peptide induces antioxidant genes and protects cells against oxidative stress. (**A**) Map of the plasmid containing the TatNrf2mer sequence. A DNA sequence coding for the HIV-1 Tat peptide fused to the Nrf2 peptide was designed and codon optimized for expression in humans and mice. This sequence was cloned in a lentiviral vector plasmid fused to the puromycin resistance gene by a T2A self-cleaving peptide sequence. (**B**) Detection of TatNrf2mer mRNA in stably transfected ARPE-19 cells expressing TatNrf2mer. ARPE-19 cells transduced with lentiviral vectors delivering either TatNrf2mer-PuroR or PuroR were selected in puromycin. Total RNA was isolated from both stable cells, and a cDNA library was generated to detect the presence of TatNrf2mer by RT-PCR. Lentiviral plasmid containing the TatNrf2mer sequence was used as a positive control. (**C**) Constitutive expression of TatNrf2mer induces the expression of ARE genes. Quantitative RT-PCR detecting the GSTM1 and NqO1 mRNA was performed using the cDNA library described in (**B**), using β-actin as a control. ARPE-19 stably expressing TatNrf2mer had greater expression of ARE genes. Assays were performed in triplicate. (**D**) TatNrf2mer expression protects ARPE-19 cells from paraquat and H_2O_2 induced oxidative stress. Stably transfected ARPE-19 cells were incubated with 55, 166, or 500 μM paraquat for 48 hours or with 800 μM H_2O_2 for 6 hours to induce oxidative damage. Afterwards, cell viability was assessed with the Cell Titration or MTT assay, respectively. Assays were performed in triplicate. Values are reported as average ± SD.

Results

Design of a Secretable and Cell-Penetrating Nrf2 Peptide

Steel et al.[23] reported an Nrf2 derived peptide that can induce the expression of antioxidant genes in vitro. We developed a DNA sequence encoding an Nrf2-derived peptide that can be delivered via AAV (Fig. 1A). Stable cell lines expressing this peptide were created following transduction of an LV expressing TatNrf2mer from the EF1α promoter. Cells expressing this peptide were selected with puromycin, because the puromycin resistance gene was linked to the Nrf2 peptide using a 2A self-cleaving peptide, permitting separation of the two proteins during translation.[38] Transcription of TatNrf2mer in a human RPE–derived cell line (ARPE-19) was confirmed by reverse transcription PCR (Fig. 1B). Retinal pigment epithelial cells stably expressing TatNrf2mer exhibited increased expression of antioxidant genes, glutathione S-transferase mu 1 (*GSTM1*) and NAD(P)H dehydrogenase quinone 1 (*NqO1*), which contain the ARE in their promoters[39] (Fig. 1C). We noted some induction of *GSTM1* in the vector-only (LV-PuroR) treated cells, which we believe is related to protein aggregation caused by the ongoing puromycin selection. Nevertheless, expression of the TatNrf2mer peptide led to higher levels of induction of this ARE gene and of *NqO1*. Cells expressing the Nrf2 peptide also showed increased resistance to oxidative injury caused by treatment with paraquat or hydrogen peroxide (Fig. 1D). Once more, we observed some protection from H_2O_2 in the vector cells; however, the cells expressing the TatNrf2mer peptide showed a much higher protection from this stress. Low levels of the mitochondrial-specific toxin paraquat killed 50% of the ARPE-19 cells, but this response was almost completely blocked by expression of TatNrf2mer.

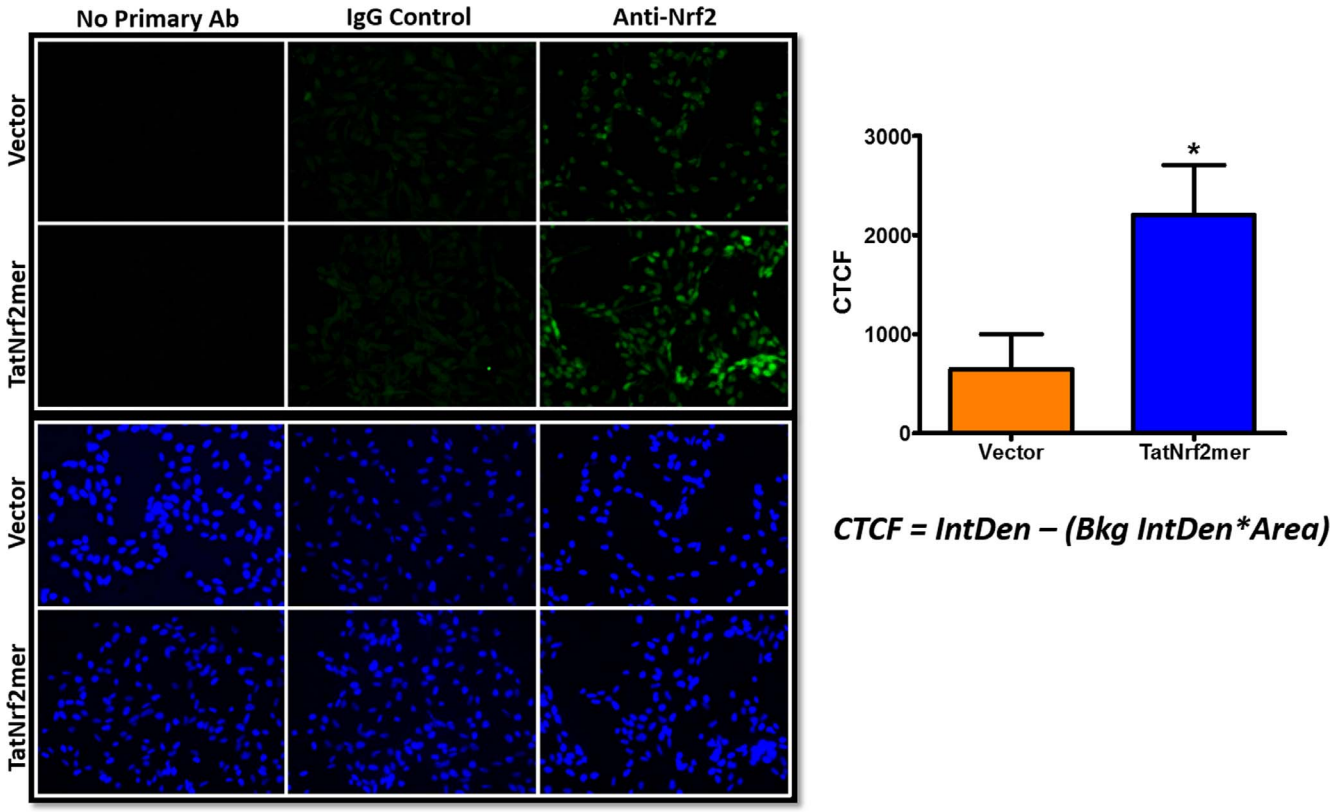

Figure 2. Expression of TatNrf2mer increases the expression of endogenous Nrf2 in ARPE-19 cells. ARPE-19 cells stably expressing either TatNrf2mer-T2A-PuroR (TatNrf2mer) or T2A-PuroR were selected by the addition of puromycin. Stably transduced cells were stained with an antibody against the Nrf2 protein. Secondary antibody conjugated to Alexa Fluor 488 chromophore (*green*) was used to detect the presence or absence of the anti-Nrf2 antibody. DNA staining with DAPI (*blue*) was used as a counter stain. An isotype control antibody was included to detect any nonspecific binding of the secondary antibody. The fluorescence intensity was quantified using ImageJ software (http://imagej.nih.gov/ij/; provided in the public domain by the National Institutes of Health, Bethesda, MD, USA) and the corrected total cell fluorescence (CTCF)[63,64] formula described on the *bar graph* on the *right*. Values are reported as average ± SD ($n = 3$ images).

Immunofluorescence was used to determine if increases in the expression of ARE genes was associated with activation of Nrf2. ARPE-19 cells stably expressing either the puromycin resistance gene (*PuroR*) only (control vector) or the TatNrf2 peptide with the PuroR (TatNrf2mer) were stained with an antibody against endogenous Nrf2 (this antibody does not detect the TatNrf2mer peptide), an isotype control antibody, or no primary antibody. Control vector treated cells showed less intense Nrf2 staining. However, TatNrf2mer-expressing cells had more intense Nrf2 staining that co-localized with DAPI-stained nuclei (Fig. 2). The IgG control antibody control confirms the specificity of the staining (Fig. 2). The level of nuclear Nrf2 stain in TatNrf2mer treated and vector-only cells was compared using ImageJ software to calculate the corrected total cell fluorescence (CTCF). To detect changes in the levels of Nrf2 in these cells, we conducted a Western blot using cell lysates and probing the membrane with an anti-Nrf2. We observed an increase signal for Nrf2 in cells expressing the TatNrf2mer (Supplementary Figs. S1A, S1B) indicating a stabilization of the Nrf2 expression in these cells. To determine any nuclear translocation of Nrf2, cells were fractionated into cytosol (cyto) and nuclear (nuc) fractions using the REAP protocol as described by Suzuki et al.[40] When the fractions were probed with the same anti-Nrf2 antibody, we observed an increased Nrf2 band density in the nuclear fraction of cells expressing the TatNrf2mer (Supplementary Figs. S1C, S1D). These results suggest that expression of TatNrf2mer stabilized Nrf2 and induced nuclear translocation of this transcription factor when TatNrf2mer was expressed within those cells.

To determine if the peptide could act on cells that did not express TatNrf2mer themselves, we further modified TatNrf2mer cDNA by fusing it to GFP rendered secretable by including an Ig_{κ} leader secretion signal upstream of the coding sequence (sGFP). A furin cleavage site (FCS) was inserted as a linker region between secretable GFP (sGFP) and TatNrf2mer. We also created a similar sequence lacking the TatNrf2mer cDNA (sGFP-FCS) and a GFP cDNA without secretion signal (Fig. 3A) as a controls. Using lentiviral vectors, we created HEK293T cells that stably express GFP, sGFP-FCS, or sGFP-FCS-TatNrf2mer. Cells transduced with sGFP-containing lentiviruses (sGFP-FCS and sGFP-FCS-TatNrf2mer) showed green fluorescence that associated with cell membranes and the extracellular space, while cells expressing nonsecretable GFP showed cytoplasmic labeling (Fig. 3B). To demonstrate the secretion and proteolysis of the sGFP-TatNrf2mer, cells expressing sGFP or sGFP-TatNrf2mer were cultivated in low protein media for 3 days. The conditioned media were harvested and concentrated using a 50 kDa cut-off concentrator (Amicon Ultra Millicell; Millipore, Billerica, MA, USA) and cells were homogenized in lysis buffer. Our Western blot detecting GFP shows that the fused sGFP-TatNrf2mer lysate had a higher molecular weight band than that present in the sGFP lysate. However, the conditioned media of both cell lines showed a band of approximately 27 kDa corresponding to the molecular weight

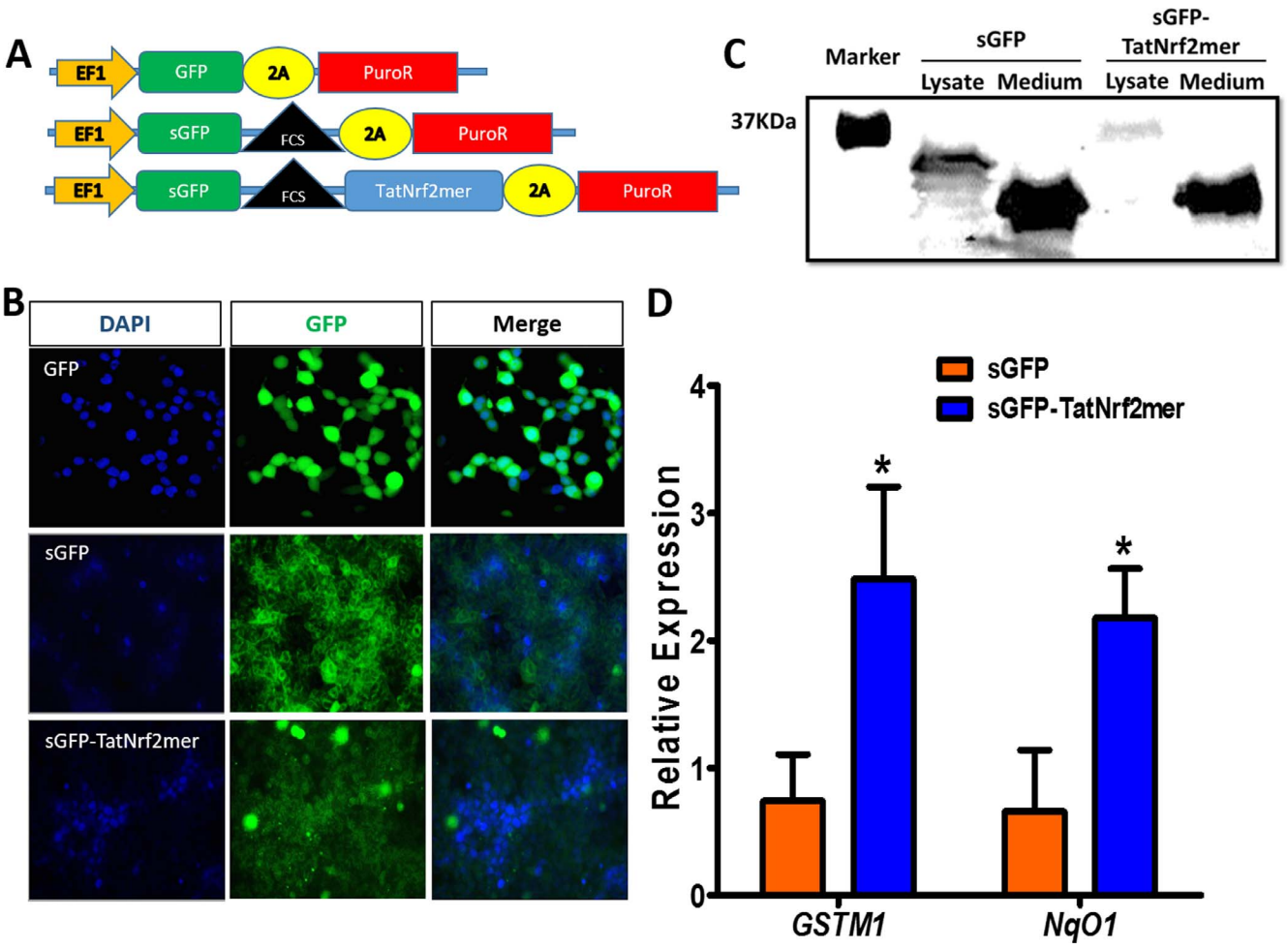

Figure 3. A secretable TatNrf2mer induces the expression of ARE genes. (**A**) Two lentiviral vectors delivering a secretable GFP (sGFP) or a sGFP fused to the TatNrf2mer by a furin cleavage site (FCS) were designed. Both constructs were cloned in-frame with the 2A-puroR sequence of the lentiviral vector to generate fusion proteins. Plasmids were packaged as lentiviral vector particles. (**B**) Distribution of GFP and sGFP-TatNrf2mer in stably transfected HEK293T cells. HEK293T cells were transduced with lentiviral vectors delivering either GFP, sGFP, or sGFP-TatNrf2mer and were selected in the presence of puromycin. The expression of GFP was evaluated by fluorescence microscopy. The sGFP and sGFP-TatNrf2mer had a different pattern of cellular distribution than the GFP expressing cells. DAPI staining was performed as a counter stain. (**C**) Stable cells were grown in low protein medium for 3 days. The conditioned media were collected and cells were lysed. The presence of GFP fused molecules was determined by Western blot using antibody to GFP. Although the sGFP-TatNrf2mer fused protein is detected in the lysate, the only band detected in the medium corresponds to cleaved GFP, thus suggesting the secretion and cleavage of the sGFP-TatNrf2mer protein. (**D**) The conditioned media from sGFP-TatNrf2mer increased the expression of two ARE genes in ARPE-19 cells. ARPE-19 cells were incubated with the 3-day conditioned media of either sGFP or sGFP-TatNrf2mer for 18 hours. Total RNA was isolated from these cells and a cDNA library was generated. The relative expression of the two ARE genes *GSTM1* and *NqO1* was measured by qRT-PCR using β-actin as a control transcript. Values are reported as average ± SD ($n = 3$ biological replicates).

of GFP (Fig. 3C), thus suggesting that the sGFP-TatNrf2mer fusion protein is being secreted and proteolyzed. Finally, to demonstrate that released TatNrf2mer can penetrate cells, ARPE-19 cells were incubated with conditioned media from sGFP-FCS or sGFP-FCS-TatNrf2mer transduced HEK293T cells. Cells treated with the sGFP-TatNrf2mer conditioned media exhibited significant increases in the expression of *GSTM1* and *NqO1* compared to cell treated with sGFP alone, suggesting that Nrf2-derived peptide was secreted from cells transduced with LV-TatNrf2mer and was able to penetrate naïve cells and activate the Nrf2 signaling (Fig. 3D). These results demonstrated that we have developed a secretable and cell penetrating Nrf2mer peptide capable of activating ARE-regulated genes. This approach provides a considerable advantage to the delivery of the naked peptide, as gene-delivery provides continuous supply of the therapeutic peptide and secretion permits a "by-stander" effect in which infected cells serve as a factory for the production of the Nrf2 peptide.

Intravitreal Injection of AAV2(quad Y-F+T-V)-smCBA-sGFP-TatNrf2 Is Safe

To promote sustained expression of a secreted Nrf2-derived peptide in the retina, we delivered it intravitreally via AAV(quad Y-F+T-V)[31] (Fig. 4A). sGFP-FCS-TatNrf2mer was cloned downstream of the chicken β actin promoter which is constitutively active within all retinal cells.[41] One month after injection we observed diffused AAV-mediated GFP expression by fluorescence funduscopy (Fig. 4B). In eyes injected with virus expressing nonsecreted GFP, we observed punctate and perivascular staining characteristic of retinal ganglion cell transduction. However, eyes injected with the

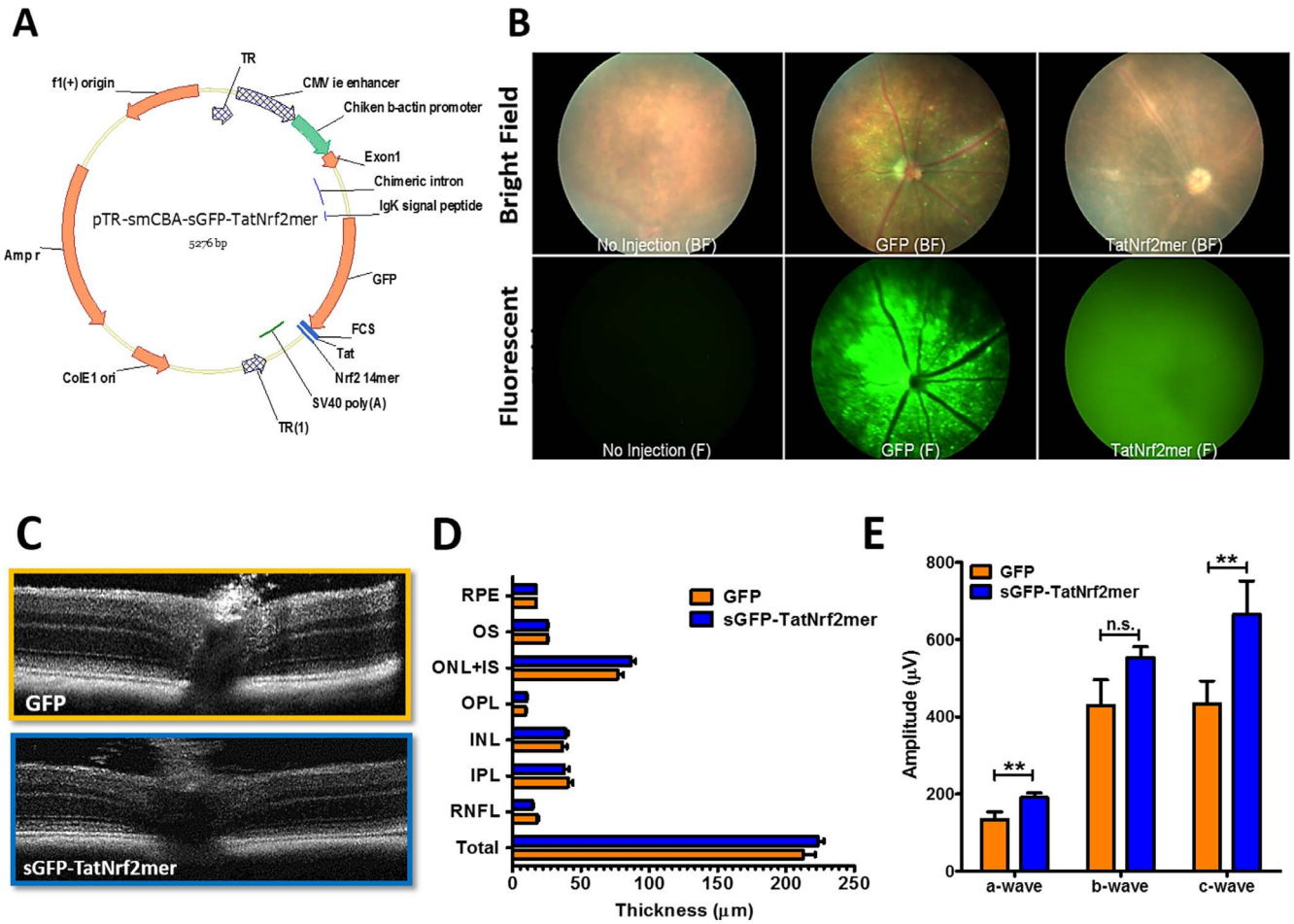

Figure 4. Expression of the sGFP-TatNrf2mer AAV vector in mice retinas is safe. (**A**) Map of the pTR-smCBA-sGFP-TatNrf2mer AAV vector. The coding sequence of the secretable and cell-penetrating peptide was cloned in an AAV plasmid containing the small CMV enhancer/chicken β-actin hybrid promoter which is constitutively active in most cells within the retina. (**B**) Expression of sGFP-TatNrf2mer gene within the retina. C57BL/6J mice were intravitreally injected with 3×10^9 vector genome copies (vgc) of AAV2-QUAD(Y-F)-T497V vector delivering either GFP or sGFP-TatNrf2mer. Three weeks after vector injection, gene expression was detected by fluorescence funduscopy. Representative fundus images demonstrate that, in contrast to the localized fluorescence expression of GFP, eyes injected with sGFP-TatNrf2mer showed a diffused fluorescence consistent with the secretion of GFP. (**C**) Two weeks after viral vector injection, mice were evaluated by SD-OCT to detect changes within the different layers of the retina. Representative images of retinas transduced with AAV vectors delivering GFP (*top*) or sGFP-TatNrf2mer (*bottom*). (**D**) Quantification of the different retina layers. The thickness of each layer was measured using the segmentation analysis of Diver 2.0 software from Bioptigen. No statistically significant difference was observed in any layer between eyes injected with GFP or sGFP-TatNrf2mer vector. (**E**) TatNrf2mer expression within the retina was not deleterious to the electrophysiological activity of the tissue. Injected mice were evaluated by ERG to detect any differences in amplitude between the expression of GFP and sGFP-TatNrf2mer. Eyes injected with the sGFP-TatNrf2mer AAV vector had statistically significant higher a-wave and c-wave amplitudes ($P < 0.05$) when compared to eyes injected with the GFP AAV vector. ERG b-wave amplitudes also were elevated but did not reach statistical significance ($P = 0.062$). Values are reported as average ± SEM ($n = 10$ mice).

sGFP-FCS-TatNrf2mer vector had a diffused pattern of GFP fluorescence. Noninjected mice exhibited no green fluorescence, confirming that the diffuse fluorescence observed in the sGFP-TatNrf2mer–treated eyes is caused by the secreted GFP and not by tissue autofluorescence.

We next sought to determine the safety of AAV-mediated sGFP-FCS-TatNrf2mer in the retina of wild type mice. The effects of our vector on the thickness of the different layers of the retina was determined using SD-OCT. Images from all eyes were acquired centered on the optic nerve head (Fig. 4C). These images were segmented into the different retina layers and the thickness of each layer was measured by using the Bioptigen Diver 2.0 software. When the average thickness of each layer was compared between eyes expressing GFP or sGFP-TatNrf2mer, no statistically significant difference was observed (Fig. 4D). These mice then were evaluated by full-field, scotopic ERG to determine if treatment impacted retinal function. By comparing the averaged maximal amplitudes of the a-, b-, and c-waves we found that retinal transduction by AAV-sGFP-TatNrf2mer significantly increased a- and c-wave, but not b-wave (Fig. 4E). These increases might reflect increased resistance of the photoreceptors (a-wave) and RPE (c-wave) to stress associated with aerobic metabolism. Together these results strongly suggest that transduction with our sGFP-TatNrf2 vector does not cause significant alterations to retinal structure or function in wild type mice. We note that a better control for this and for subsequent experiments would have been to use AAV expressing secreted GFP rather than intracellular GFP, but our intent was to control for the potential protective effects intraocular injections, which induce the production of neurotrophic factors.[42]

Investigative Ophthalmology & Visual Science

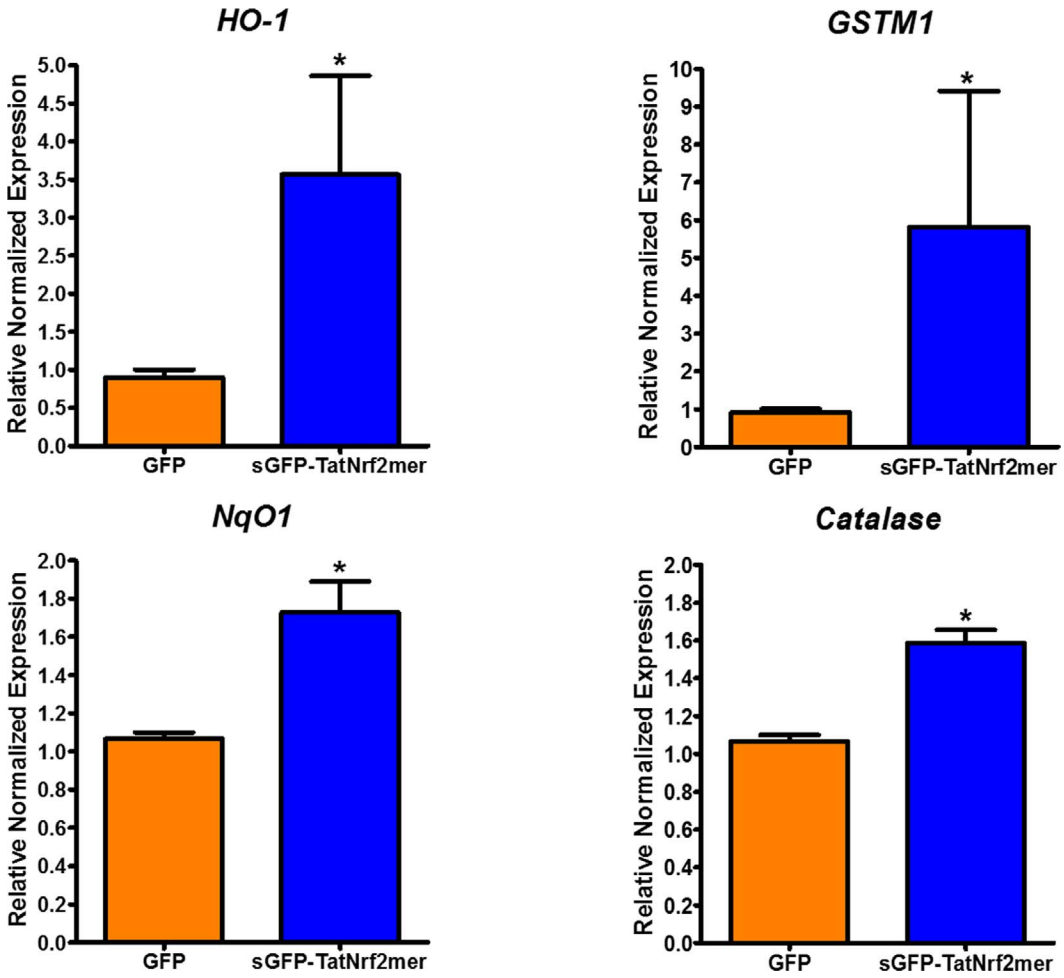

Figure 5. Gene delivery of TatNrf2mer increases the expression of antioxidant genes within the retina. C57BL/6J mice were injected intravitreally with 3×10^9 vgc/eye of AAV2-QUAD(Y-F) T497V delivering either GFP or sGFP-TatNrf2mer. One month after the injection, mice were euthanized, their retinas were harvested, and RNA isolated from them. A cDNA library from each treatment was prepared and qRT-PCR was performed to measure the relative levels of the ARE genes *HO-1* and *GSTM1* using β-actin as a control. Eyes treated with the sGFP-TatNrf2mer vector had higher levels of *HO-1*, *GSMT1*, *NqO1*, and *Catalase* (all antioxidant genes) when compared to GFP injected control eyes. Values are reported as average ± SEM ($n = 5$ biological samples).

Intravitreal Delivery of AAV-sGFP-TatNrf2mer Protects the Retina Against Oxidative Stress

Knowing that AAV-sGFP-TatNrf2mer caused no overt retinal damage when delivered intravitreally, we next asked if the same dose of vector could induce the expression of *ARE* genes within the retina. C57BL/6J were injected intravitreally as in the previous experiment, and the expression of *ARE* genes was measured by qRT-PCR. In neural retinas of eyes injected in the vitreous with AAV-sGFP-TatNrf2mer we observed an increase in the expression of *HO-1*, *GSTM1*, *NqO1*, and *catalase* relative to AAV-GFP treated eyes (Fig. 5). The level of induction among the four genes differed, suggesting that regulators other than Nrf2 impact the expression of these genes. *NqO1*, for example, also is under control of the aryl hydrocarbon receptor.[43] Still, even in the absence of acute oxidative stress, expression of TatNrf2mer led to increased expression of antioxidant genes.

To determine whether upregulation of ARE genes could protect the retina from oxidative stress, we evaluated treatment in the sodium iodate-inducible model of oxidative injury to the RPE.[44] Mice were injected intravitreally in one eye with AAV-GFP and with AAV-sGFP-TatNrf2mer in the contralateral eye. One month later, IP injections of $NaIO_3$ (35 mg/kg) were administered and, 1 week later, retinal function was evaluated by full field scotopic ERG. Eyes treated with AAV-sGFP-TatNrf2mer showed a partial protection of the ERG *a*- and *b*- wave amplitudes, suggesting protection of the photoreceptors and bipolar cells (Figs. 6A, 6B). However, there was no protection of the c-wave amplitude relative to control-treated contralateral control eyes at this dose (Fig. 6C). We decided to test a lower dose of $NaIO_3$ to determine if it is possible to protect the c-wave from a less severe injury. A second cohort treated with our vectors were injected IP with 25 mg/kg $NaIO_3$ and 7 days later were evaluated by ERG. In this cohort we also observed a protection of a- and b-wave (Figs. 6D, 6E), but this group of animals also showed a slight but significant protection of the c-wave (Fig. 6F).

Next, we sought to determine if this protection of the ERG at the lower dose of $NaIO_3$ was associated with a protection of the retinal structure. Mice were evaluated by SD-OCT at day 9 after injection with $NaIO_3$. The thickness of the whole retina, the inner nuclear layer (INL), and the outer nuclear layer (ONL) was performed on SD-OCT images. Animals expressing the sGFP-TatNrf2mer showed a significantly thicker ONL when compared to GFP-treated control eyes (Supplementary Fig.

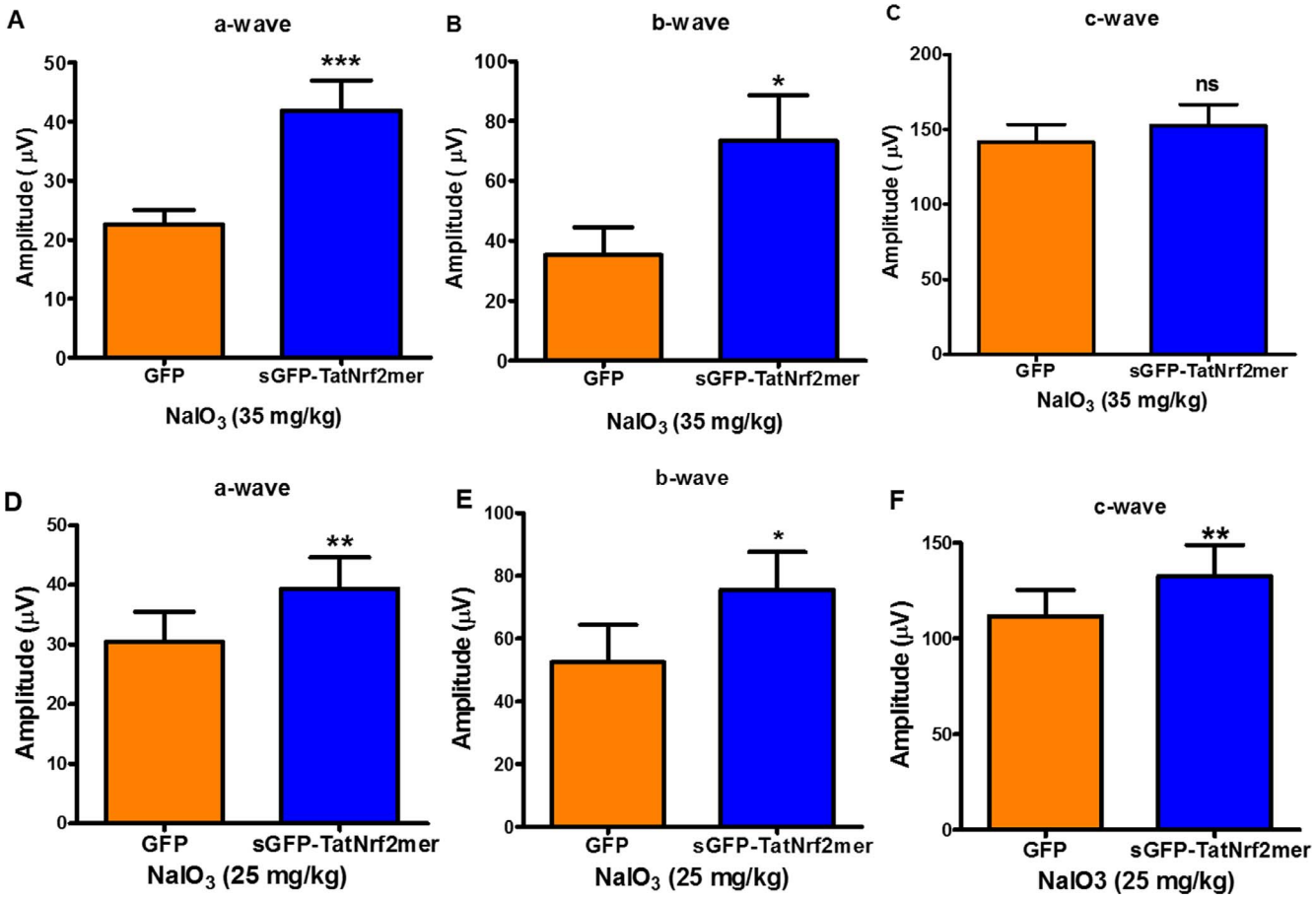

Figure 6. Expression of sGFP-TatNrf2mer partially protects the electrical activity of the retina from acute oxidative damage of $NaIO_3$. C57BL/6J mice were injected with the AAV vectors described in previous figures. One month after the intravitreal injection of the vector, mice were injected intraperitoneally with 35 mg/kg sodium iodate to induce oxidative stress within the RPE. Seven days later mice were evaluated by ERG. One week after $NaIO_3$ injury, eyes injected with the sGFP-TatNrf2mer had partial protection of the ERG a-wave (**A**) and b-wave (**B**) but not c-wave ($P = 0.20$; [**C**]), when compared to GFP injected eyes. (**D–F**) A second group of mice treated with the same AAV vectors received $NaIO_3$ at a lower dose (25 mg/kg) and evaluated as in the first cohort. At this lower dose, the amplitude of all the waves was significantly higher among the eyes treated with the sGFP-TatNrf2mer. Histograms report the maximum amplitudes recorded at 0 dB using the UTAS BigShot Visual Diagnostic System (2.7 cd.s/m^2). Values are reported as average ± SEM ($n = 11$ mice in first cohort, $n = 9$ mice in second cohort).

S2A), though overall retinal thickness and INL thickness were not affected. To determine if TatNrf2mer-treated eye showed lower levels of oxidative stress compared to GFP-expressing eyes, the retinas were harvested and the amounts of nitrotyrosine (a marker of protein oxidation) were quantified. Our results showed that eyes treated with the sGFP-TatNrf2mer vector a greater than 50% reduction in the level of nitrotyrosine-modified proteins when compared to eyes treated with AAV-GFP (Supplementary Fig. S2B). Finally, because of the partial protection of the c-wave among these animals we examined the effects on RPE architecture by RPE flat mount. Immunofluorescence analyses (ZO-1 staining) of the RPE layer revealed comparable damage to the RPE structure in AAV-GFP and AAV-sGFP-TatNrf2mer–treated eyes (Supplementary Fig. S2C). However, at higher magnification (×20), we observe some preservation of the RPE cells structure in the eyes treated with the AAV-sGFP-TatNrf2mer when compared to AAV-GFP treated eyes, which exhibited many distorted and enlarged RPE cells. These results indicated that our TatNrf2mer vector did not completely protect the RPE but did modulate the Nrf2 signaling pathway in the retina and, in so doing, protected the retina from oxidative stress.

AAV-sGFP-TatNrf2mer Protects the Retina Against Intraocular Inflammation

Current research associates dry-AMD with oxidative stress and inflammation.[45–48] We, therefore, tested the effect of intravitreal AAV-sGFP-TatNrf2mer on the modulation of proinflammatory signals in the $NaIO_3$-treated mice. In retina and RPE extracts, we found that eyes treated with AAV-sGFP-TatNrf2mer had significantly lower quantities of IL-1β and IL-6 following $NaIO_3$ exposure (Fig. 7). The specificity of this effect was demonstrated by a lack of significant changes in the MCP-1 (Ccl2) chemokine. This result suggested that the AAV-sGFP-TatNrf2mer vector has anti-inflammatory properties in the face of acute oxidative stress.

The reduction of IL-1β level suggests an inhibition of the inflammasome signaling that regulates the activation and secretion of this cytokine, which is produced in response to signaling by the NLRP3 inflammasome. Inflammasome activation recently has been associated with dry-AMD.[49] To test this hypothesis in vitro, we challenged stably transfected ARPE-19 cells expressing either LV-Puro or LV-TatNrf2mer-PuroR with the reactive aldehyde 4-hydroxynonenal (4-HNE), which is known to accumulate in eyes donated by patients

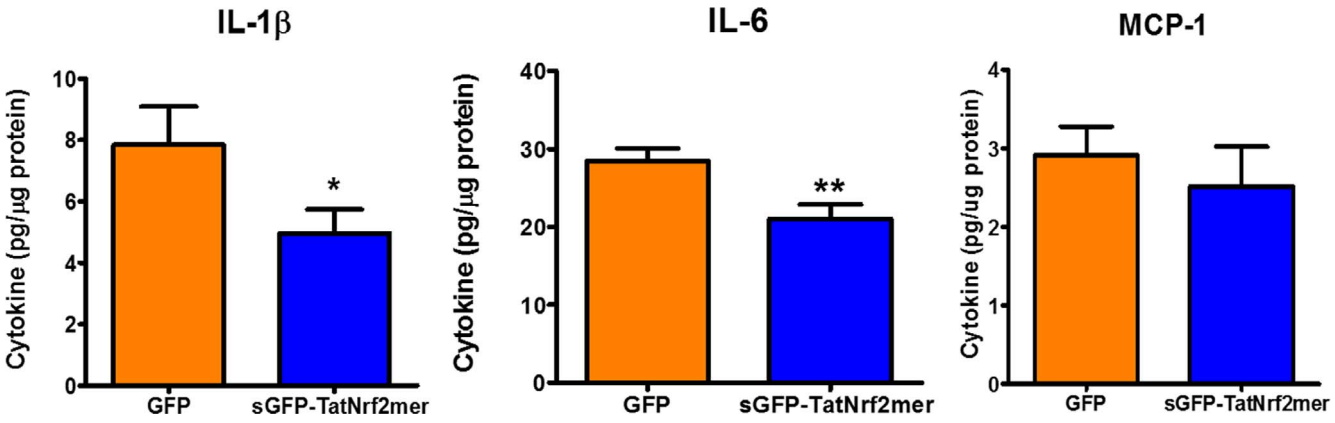

Figure 7. The secretable TatNrf2mer decreases inflammatory cytokines in the retinas of $NaIO_3$ treated mice. Retinas and RPE from mice treated with 25 mg/kg $NaIO_3$ were harvested and sonicated in PBS supplemented with protease inhibitors. The protein concentration in the cleared lysate was determined and diluted to 400 ng/mL protein. The concentration of IL-1β, IL-6, and MCP-1 were determined by ELISA using 10 μg total protein per sample. Biological samples were evaluated in triplicates. Values are reported as average ± SEM ($n = 7$ samples).

with AMD.[11] Treatment of control cells (LV-Puro) with 4-HNE led to a 12-fold increase in IL-1β secretion, but cells expressing TatNrf2mer peptide did not secrete significant amounts of IL-1β into the media (Fig. 8A). This finding suggested that TatNrf2mer can inhibit the inflammasome signaling pathway. To test the effect of the AAV-sGFP-TatNrf2mer on the recruitment of inflammatory cells, we used the EIU mouse model[50] as described in the Materials and Methods section. Mice were treated with AAV-GFP in one eye and with AAV-sGFP-TatNrf2mer in the other, as in the

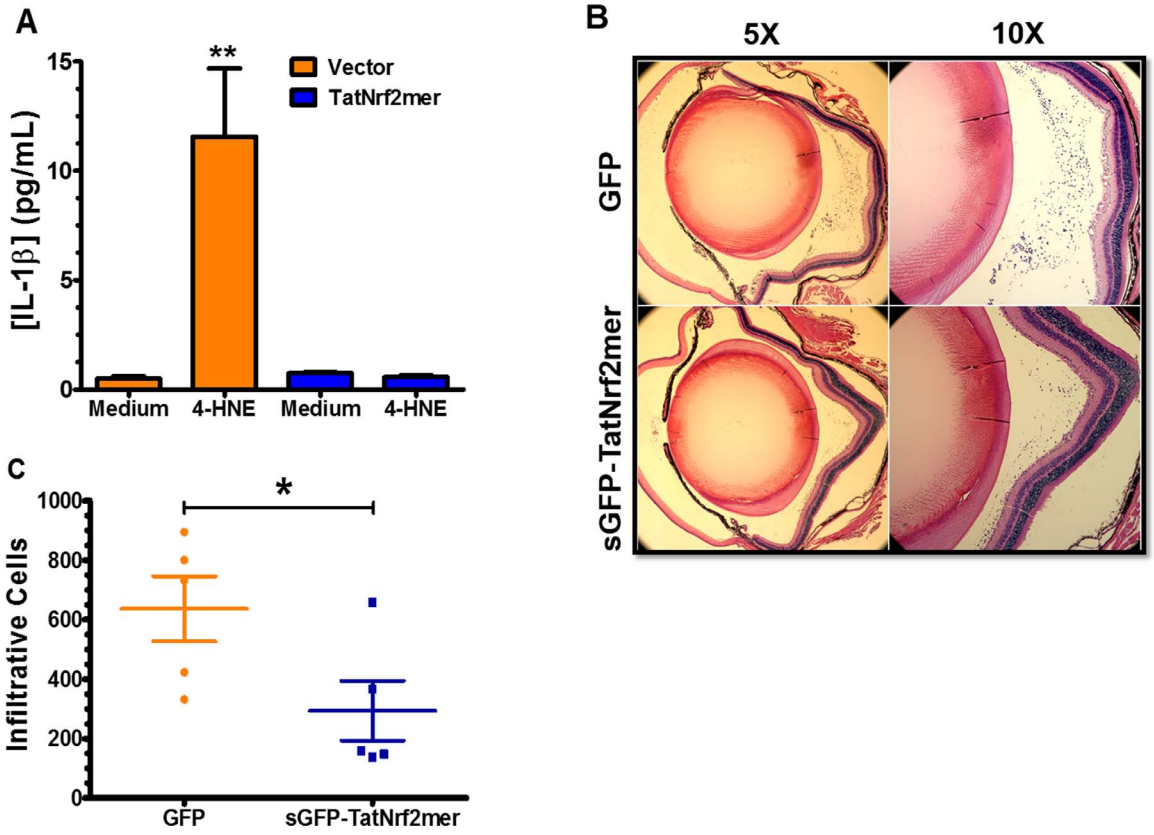

Figure 8. The secretable TatNrf2mer has anti-inflammatory properties in a mouse model of ocular inflammation. (**A**) ARPE-19 stably expressing PuroR (Vector) or TatNrf2mer-PuroR (TatNrf2mer) were incubated with or without 30 μM 4-hydroxynonenal (4-HNE) for 18 hours. The concentration of IL-1β in the conditioned media was quantified in triplicate by ELISA. (**B**) C57BL/6J mice were injected intravitreally with 3×10^9 vgc of AAV vector delivering either GFP or sGFP-TatNrf2mer (TatNrf2mer). One month later mice were injected intravitreally with 25 ng LPS and then were euthanized 24 hours later. Their eyes were harvested and analyzed by histology. Representative images of hematoxylin and eosin–stained sections of eyes injected with either GFP (*top*) or TatNrf2mer vectors are shown (*bottom*). (**C**) The number of cells within the vitreous of at least two sections per eye were quantified by two independent subjects who were not aware of the treatments. Eyes injected with the TatNrf2mer AAV vector had significantly lower numbers of infiltrating cells within the vitreous body than the eyes injected with the GFP AAV vector. Values are reported as average ± SEM ($n = 2$ biologic replicates in [**A**], $n = 5$ mice in [**C**]).

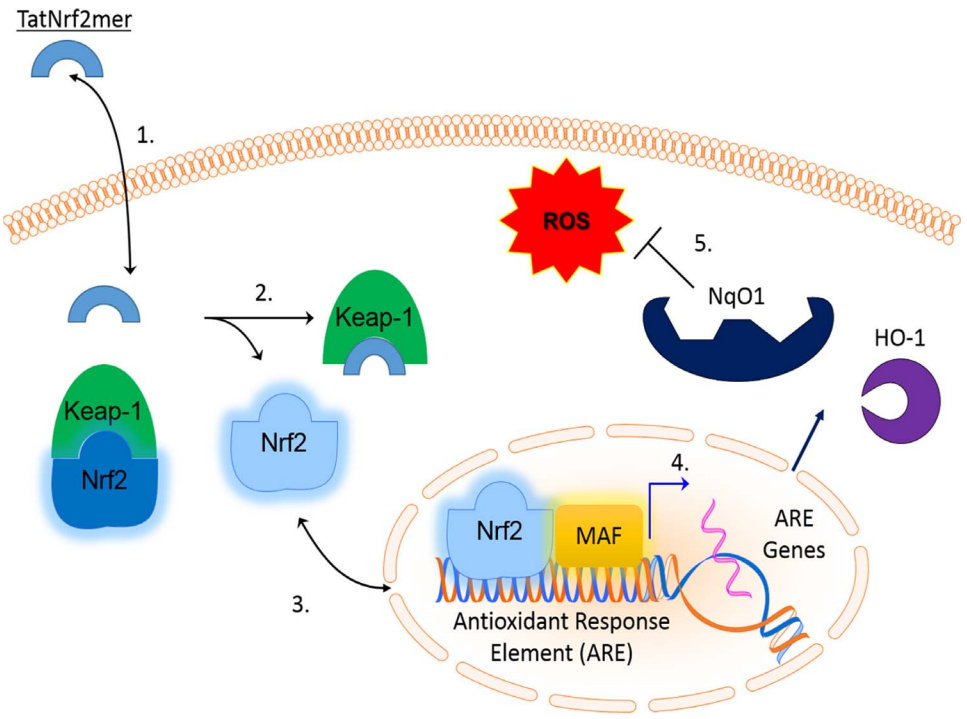

Figure 9. Mechanism of action of TatNrf2mer. The Nrf2mer peptide is derived from the *Nrf2* gene domain that binds Keap-1 and penetrates cells when fused to the Tat peptide. Once inside the cell, the TatNrf2mer binds to Keap-1 liberating *Nrf2*, which can translocate into the nucleus where it induces the expression of antioxidant genes (e.g., *NqO1* and *HO-1*). These genes then reduce the ROS within therefore protecting the cell from the deleterious effects of free radicals.

oxidative stress experiments. One month later, they were injected in both eyes with *E. coli* lipopolysaccharide, euthanized 24 hours later, and their eyes harvested and fixed for histologic analysis (Fig. 8B). The number of infiltrating cells within the vitreous was quantified by two independent masked observers, and it was determined that eyes treated with the TatNrf2mer AAV vector showed significantly fewer infiltrating cells within the vitreous body (Fig. 8C). These results confirmed that AAV-sGFP-TatNrf2mer has anti-inflammatory properties in the eye.

Discussion

We developed an AAV vector that produces a secreted Nrf2 peptide with cell-penetrating properties. We demonstrated that our TatNrf2mer construct can induce the nuclear translocation of endogenous Nrf2 based on immunofluorescence and biochemical studies. Nuclear import of Nrf2 resulted in the expression of ARE genes in vitro and in vivo when measured by qRT-PCR. Furthermore, expression of our TatNrf2mer sequence was sufficient to protect cells from the damaging effects of potent oxidants, paraquat and H_2O_2 (by measuring cell viability in vitro) and $NaIO_3$ (by measuring the electrophysiological response of the retina in vivo). We note that RPE cells were protected from oxidative damage in vitro (Figs. 1, 3C), but were not fully protected in the $NaIO_3$ injury model in mice. There are several potential explanations for this discrepancy. It is possible that the peptide did not reach the RPE following intravitreal injection of the virus. However, this protein (2.95 kDal) is much smaller than ranibizumab (48.3 kDal) which effectively blocks choroidal neovascularization following intravitreal injection. Another interpretation is that the virally delivered peptide was not sufficient to protect the RPE in this severe model of acute oxidative stress. We currently are attempting to distinguish between these alternatives by measuring TatNrf2mer protein levels in the neural retina and RPE and by testing AAV-sGFP-TatNrf2mer in a model of chronic RPE oxidative stress.[51] When tested in models of inflammation, expression of TatNrf2mer significantly inhibited the secretion of IL-1β in vitro and LPS-induced recruitment of inflammatory cells within the vitreous humor of mice.

Our data suggested the following steps in the function of our AAV-delivered Nrf2 peptide (Fig. 9): (1) Secreted TatNrf2mer penetrates nearby cells by virtue of its Tat-peptide sequence, (2) intracellular TatNrf2mer liberates endogenous Nrf2 from Keap1, (3) Nrf2 translocates to the nucleus and induces the expression of ARE genes, (4) these ARE genes are translated into the active enzymes within the cytoplasm of the cells, and (5) active antioxidant enzymes reduce the burden of ROS, thereby protecting the cells.

Although important for cell signaling events, when produced in excess, ROS can damage otherwise stable macromolecules, particularly membrane lipids. This process can lead to the generation of DAMP molecules that often trigger an inflammatory response accelerating the progression of the disease. Furthermore, increased mitochondrial oxidative stress can be sensed by the thioredoxin interacting protein (TXNIP) which can lead to activation of the inflammasome and to a proinflammatory response.[52–54] The Nrf2 response can reduce the level of ROS, by increasing the level of antioxidant enzymes, such as heme oxygenase, catalase, and NqO1, and it can dampen inflammatory signaling by regenerating thioredoxin.[55] These mechanisms are of importance in tissues with a high metabolic rate, such as the retina.

Photo-oxidative damage to the RPE has been experimentally linked to AMD.[56,57] Brandstetter et al.[58] provided an explanation of how exposure to high intensity light and accumulation

Investigative Ophthalmology & Visual Science

of lipofuscin could affect RPE viability. Interestingly, the combination of oxidative stress and modified photoreceptor outer segments resulted not only in cell death, but also in the activation of the inflammasome and secretion of IL-1β and IL-18. These cytokines also have been implicated in other ocular diseases, such as proliferative diabetic retinopathy and polypoidal choroidal vasculopathy.[59–62]

Our work characterized a novel method for the delivery of small peptides within the retina using AAV vectors. By transducing cells within the retina with a gene encoding the Nrf2 peptide that can be secreted and taken up by other cells, we bypassed the need for the repeated administration of such peptides. Furthermore, the secretory and cell-penetrating properties of our gene transfer approach potentially allows the use of a lower dose of vector to achieve therapeutic effects due to its "by-stander" effect when compared to a cell-autonomous version of the peptide. As noted above, Xiong et al.[19] showed that increasing Nrf2 expression via subretinal injection of AAV8-Nrf2 improved the electrophysiological response and the visual acuity in a mouse model of inherited retinal degeneration. While subretinal injection currently is used in clinical trials for gene therapy, the injection of a virus producing a secretable peptide is more readily translatable to clinical practice, because intravitreal injection of the virus should permit the distribution of the short peptide to all layers of the neural retina and to the RPE. In addition, in a clinical setting intravitreal administration is less intrusive than the subretinal injection.

Besides its antioxidant properties, our vector seems to possess the added benefit of being anti-inflammatory. Our AAV-sGFP-TatNrf2mer vector decreased the IL-1β and IL-6 cytokines in the retinas of $NaIO_3$ treated mice. Furthermore, when tested in the routinely used EIU mouse model, AAV-sGFP-TatNrf2mer decreased inflammation associated with the intravitreal delivery of LPS. We currently are developing methods for analyzing multiple cytokines in vitreous humor extracts. We also are aware of one potential limitation of this technology for the treatment of ocular disease, the possibility that constitutive suppression of the inflammatory response may make the posterior chamber more sensitive to infection. Before clinical application, emphasis should be placed on methods to regulate expression of secreted TatNrf2mer and on dose-response. Nevertheless, oxidative stress and inflammation are associated diseases, such as Alzheimer's disease and ALS, and, therefore, the vector characterized herein could be of significant use within and outside the eye.

Acknowledgments

The authors thank Vince Chiodo from the Retina Gene Therapy Vector Core for production of AAV vectors, and James Thomas for his assistance in the large-scale preparation of DNA.

Supported by a grant from the National Eye Institute (NEI; Bethesda, MD; R01 EY02025), a grant from the Florida Biomedical Research Foundation (e-10KG-s), a grant from the Macula Vision Research Foundation, an AMD Research Fellowship from ARVO/Genentech, and the Shaler Richardson Professorship endowment. Core facilities were supported by NEI Grant P30 EY02172.

Disclosure: **C.J. Ildefonso**, P; **H. Jaime**, None; **E.E. Brown**, None; **R. Iwata**, None; **C. Ahmed**, None; **M. Massengill**, None; **M.R. Biswal**, None; **S.E. Boye**, None; **W.W. Hauswirth**, AGTC, Inc. (I); **J.D. Ash**, None; **Q. Li**, P; **A.S. Lewin**, P

References

1. Ikawa M, Okazawa H, Tsujikawa T, et al. Increased oxidative stress is related to disease severity in the ALS motor cortex: a PET study. *Neurology*. 2015;84:2033–2039.
2. Carrì MT, Valle C, Bozzo F, Cozzolino M. Oxidative stress and mitochondrial damage: importance in non-SOD1 ALS. *Front Cell Neurosci*. 2015;9:41.
3. Hollyfield JG, Bonilha VL, Rayborn ME, et al. Oxidative damage-induced inflammation initiates age-related macular degeneration. *Nat Med*. 2008;14:194–198.
4. Beatty S, Koh HH, Phil M, Henson D, Boulton M. The role of oxidative stress in the pathogenesis of age-related macular degeneration. *Surv Ophthalmol*. 2000;45:115–134.
5. Hollyfield JG. Age-related macular degeneration: the molecular link between oxidative damage, tissue-specific inflammation and outer retinal disease: the Proctor lecture. *Invest Ophthalmol Vis Sci*. 2010;51:1275–1281.
6. Gao H-M, Zhou H, Hong J-S. NADPH oxidases: novel therapeutic targets for neurodegenerative diseases. *Trends Pharmacol Sci*. 2012;33:295–303.
7. Uchida K. Aldehyde adducts generated during lipid peroxidation modification of proteins. *Free Radic Res*. 2015;49:896–904.
8. Terluk MR, Kapphahn RJ, Soukup LM, et al. Investigating mitochondria as a target for treating age-related macular degeneration. *J Neurosci*. 2015;35:7304–7311.
9. Ethen CM, Reilly C, Feng X, Olsen TW, Ferrington DA. Age-related macular degeneration and retinal protein modification by 4-hydroxy-2-nonenal. *Invest Ophthalmol Vis Sci*. 2007;48:3469–3479.
10. Hollyfield JG, Perez VL, Salomon RG. A hapten generated from an oxidation fragment of docosahexaenoic acid is sufficient to initiate age-related macular degeneration. *Mol Neurobiol*. 2010;41:290–298.
11. Handa JT. How does the macula protect itself from oxidative stress? *Mol Aspects Med*. 2012;33:418–435
12. Huang HC, Nguyen T, Pickett CB. Regulation of the antioxidant response element by protein kinase C-mediated phosphorylation of NF-E2-related factor 2. *Proc Natl Acad Sci U S A*. 2000;97:12475–12480.
13. Kovac S, Angelova PR, Holmström KM, Zhang Y, Dinkova-Kostova AT, Abramov AY. Nrf2 regulates ROS production by mitochondria and NADPH oxidase. *Biochim Biophys Acta*. 2015;1850:794–801.
14. Itoh K, Wakabayashi N, Katoh Y, et al. Keap1 represses nuclear activation of antioxidant responsive elements by Nrf2 through binding to the amino-terminal Neh2 domain. *Genes Dev*. 1999;13:76–86.
15. González-Rodríguez Á, Reibert B, Amann T, Constien R, Rondinone CM, Valverde ÁM. In vivo siRNA delivery of Keap1 modulates death and survival signaling pathways and attenuates concanavalin-A-induced acute liver injury in mice. *Dis Model Mech*. 2014;7:1093–1100.
16. Jang M, Cho I-H. Sulforaphane ameliorates 3-nitropropionic acid-induced striatal toxicity by activating the Keap1-Nrf2-ARE pathway and inhibiting the MAPKs and NF-κB pathways. *Mol Neurobiol*. 2015:1–17.
17. Pan H, He M, Liu R, Brecha NC, Yu ACH, Pu M. Sulforaphane protects rodent retinas against ischemia-reperfusion injury through the activation of the Nrf2/HO-1 antioxidant pathway. *PLoS One*. 2014;9:e114186.
18. Zhao X-D, Zhou Y-T, Lu X-J. Sulforaphane enhances the activity of the Nrf2–ARE pathway and attenuates inflammation in OxyHb-induced rat vascular smooth muscle cells. *Inflamm Res*. 2013;62:857–863.
19. Xiong W, MacColl Garfinkel AE, Li Y, Benowitz LI, Cepko CL. NRF2 promotes neuronal survival in neurodegeneration and acute nerve damage. *J Clin Invest*. 2015;125:1433–1445.
20. Sachdeva MM, Cano M, Handa JT. Nrf2 signaling is impaired in the aging RPE given an oxidative insult. *Exp Eye Res*. 2014;119:111–114.

21. Nagai N, Thimmulappa RK, Cano M, et al. Nrf2 is a critical modulator of the innate immune response in a model of uveitis. *Free Radic Biol Med*. 2009;47:300–306.
22. Hancock R, Bertrand HC, Tsujita T, et al. Peptide inhibitors of the Keap1–Nrf2 protein–protein interaction. *Free Radic Biol Med*. 2012;52:444–451.
23. Steel R, Cowan J, Payerne E, O'Connell MA, Searcey M. Anti-inflammatory effect of a cell-penetrating peptide targeting the Nrf2/Keap1 interaction. *ACS Med Chem Lett*. 2012;3:407–410.
24. Boye SE, Boye SL, Lewin AS, Hauswirth WWA. Comprehensive review of retinal gene therapy. *Mol Ther*. 2013;21:509–519.
25. Jacobson SG, Cideciyan AV, Ratnakaram R, et al. Gene therapy for Leber congenital amaurosis caused by RPE65 mutations: safety and efficacy in 15 children and adults followed up to 3 years. *Arch Ophthalmol*. 2012;130:9–24.
26. Jacobson SG, Acland GM, Aguirre GD, et al. Safety of recombinant adeno-associated virus type 2–RPE65 vector delivered by ocular subretinal injection. *Mol Ther*. 2006;13:1074–1084.
27. Grote A, Hiller K, Scheer M, et al. JCat: a novel tool to adapt codon usage of a target gene to its potential expression host. *Nucleic Acids Res*. 2005;33(suppl 2):W526–W531.
28. Ildefonso CJ, Jaime H, Rahman MM, et al. Gene delivery of a viral anti-inflammatory protein to combat ocular inflammation. *Hum Gene Ther*. 2015;26:59–68.
29. Sanger F, Coulson AR. A rapid method for determining sequences in DNA by primed synthesis with DNA polymerase. *J Mol Biol*. 1975;94:441–448.
30. Zolotukhin S, Potter M, Zolotukhin I, et al. Production and purification of serotype 1, 2, and 5 recombinant adeno-associated viral vectors. *Methods*. 2002;28:158–167.
31. Kay CN, Ryals RC, Aslanidi GV, et al. Targeting photoreceptors via intravitreal delivery using novel, capsid-mutated AAV vectors. *PLoS One*. 2013;8:e62097.
32. Reed SE, Staley EM, Mayginnes JP, Pintel DJ, Tullis GE. Transfection of mammalian cells using linear polyethylenimine is a simple and effective means of producing recombinant adeno-associated virus vectors. *J Virol Methods*. 2006;138:85–98.
33. Livak KJ, Schmittgen TD. Analysis of relative gene expression data using real-time quantitative PCR and the 2(-Delta Delta C(T)) method. *Methods San Diego Calif*. 2001;25:402–408.
34. Ildefonso CJ, Jaime H, Biswal MR, et al. Gene therapy with the caspase activation and recruitment domain reduces the ocular inflammatory response. *Mol Ther J Am Soc Gene Ther*. 2015;23:875–884.
35. Justilien V, Pang J-J, Renganathan K, et al. SOD2 knockdown mouse model of early AMD. *Invest Ophthalmol Vis Sci*. 2007;48:4407–4420.
36. Mao H, James T, Schwein A, et al. AAV delivery of wild-type rhodopsin preserves retinal function in a mouse model of autosomal dominant retinitis pigmentosa. *Hum Gene Ther*. 2011;22:567–575.
37. Biswal MR, Prentice HM, Dorey CK, Blanks JC. A hypoxia-responsive glial cell-specific gene therapy vector for targeting retinal neovascularization. *Invest Ophthalmol Vis Sci*. 2014;55:8044–8053.
38. Ryan MD, Drew J. Foot-and-mouth disease virus 2A oligopeptide mediated cleavage of an artificial polyprotein. *EMBO J*. 1994;13:928–933.
39. Johnson JA, Johnson DA, Kraft AD, et al. The Nrf2-ARE pathway: an indicator and modulator of oxidative stress in neurodegeneration. *Ann N Y Acad Sci*. 2008;1147:61–69.
40. Suzuki K, Bose P, Leong-Quong RY, Fujita DJ, Riabowol K. REAP: a two minute cell fractionation method. *BMC Res Notes*. 2010;3:294.
41. Koilkonda RD, Hauswirth WW, Guy J. Efficient expression of self-complementary AAV in ganglion cells of the ex vivo primate retina. *Mol Vis*. 2009;15:2796–2802.
42. Wen R, Song Y, Cheng T, et al. Injury-induced upregulation of bFGF and CNTF mRNAS in the rat retina. *J Neurosci*. 1995;15:7377–7385.
43. Wang L, He X, Szklarz GD, Bi Y, Rojanasakul Y, Ma Q. The aryl hydrocarbon receptor interacts with nuclear factor erythroid 2-related factor 2 to mediate induction of NAD(P)H:quinone-neoxidoreductase 1 by 2,3,7,8-tetrachlorodibenzo-p-dioxin. *Arch Biochem Biophys*. 2013;537:31–38.
44. Enzmann V, Row BW, Yamauchi Y, et al. Behavioral and anatomical abnormalities in a sodium iodate-induced model of retinal pigment epithelium degeneration. *Exp Eye Res*. 2006;82:441–448.
45. Ozaki E, Campbell M, Kiang A-S, Humphries M, Doyle SL, Humphries P. Inflammation in age-related macular degeneration. In: Ash JD, Grimm C, Hollyfield JG, Anderson RE, LaVail MM, Rickman CB, eds. *Retinal Degenerative Diseases*. New York, NY: Springer; 2014:229–235.
46. Campbell M, Doyle SL. An eye on the future of inflammasomes and drug development in AMD. *J Mol Med*. 2013;91:1059–1070.
47. Ambati J, Fowler BJ. Mechanisms of age-related macular degeneration. *Neuron*. 2012;75:26–39.
48. Ambati J, Atkinson JP, Gelfand BD. Immunology of age-related macular degeneration. *Nat Rev Immunol*. 2013;13:438–451.
49. Celkova L, Doyle SL, Campbell M. NLRP3 inflammasome and pathobiology in AMD. *J Clin Med*. 2015;4:172–192.
50. Yadav UC, Ramana KV. Endotoxin-induced uveitis in rodents. *Methods Mol Biol*. 2013;1031:155–162.
51. Mao H, Seo SJ, Biswal MR, et al. Mitochondrial oxidative stress in the retinal pigment epithelium leads to localized retinal degeneration. *Invest Ophthalmol Vis Sci*. 2014;55:4613–4627.
52. Zhou R, Tardivel A, Thorens B, Choi I, Tschopp J. Thioredoxin-interacting protein links oxidative stress to inflammasome activation. *Nat Immunol*. 2010;11:136–140.
53. Devi TS, Lee I, Hüttemann M, Kumar A, Nantwi KD, Singh LP. TXNIP links innate host defense mechanisms to oxidative stress and inflammation in retinal Muller glia under chronic hyperglycemia: implications for diabetic retinopathy. *Exp Diabetes Res*. 2012;2012:438238.
54. El-Azab MF, Baldowski BRB, Mysona BA, et al. Deletion of thioredoxin-interacting protein preserves retinal neuronal function by preventing inflammation and vascular injury. *Br J Pharmacol*. 2014;171:1299–1313.
55. Dinkova-Kostova AT, Abramov AY. The emerging role of Nrf2 in mitochondrial function. *Free Radic Biol Med*. 2015;88:179–188.
56. Davies S, Elliott MH, Floor E, et al. Photocytotoxicity of lipofuscin in human retinal pigment epithelial cells. *Free Radic Biol Med*. 2001;31:256–265.
57. Rózanowska M, Jarvis-Evans J, Korytowski W, Boulton ME, Burke JM, Sarna T. Blue light-induced reactivity of retinal age pigment. In vitro generation of oxygen-reactive species. *J Biol Chem*. 1995;270:18825–18830.
58. Brandstetter C, Mohr LKM, Latz E, Holz FG, Krohne TU. Light induces NLRP3 inflammasome activation in retinal pigment epithelial cells via lipofuscin-mediated photooxidative damage. *J Mol Med*. 2015;93:905–916.
59. Miao H, Tao Y, Li X. Inflammatory cytokines in aqueous humor of patients with choroidal neovascularization. *Mol Vis*. 2012;18:574–580.
60. Ongkosuwito JV, Feron EJ, Doornik CE van, et al. Analysis of immunoregulatory cytokines in ocular fluid samples from patients with uveitis. *Invest Ophthalmol Vis Sci*. 1998;39:2659–2665.

Investigative Ophthalmology & Visual Science

61. Zhou J, Wang S, Xia X. Role of intravitreal inflammatory cytokines and angiogenic factors in proliferative diabetic retinopathy. *Curr Eye Res*. 2012;37:416–420.

62. Zhao M, Bai Y, Xie W, et al. Interleukin-1β level is increased in vitreous of patients with neovascular age-related macular degeneration (nAMD) and polypoidal choroidal vasculopathy (PCV). *PLoS One*. 2015;10:e0125150.

63. Burgess A, Vigneron S, Brioudes E, Labbé J-C, Lorca T, Castro A. Loss of human Greatwall results in G2 arrest and multiple mitotic defects due to deregulation of the cyclin B-Cdc2/PP2A balance. *Proc Natl Acad Sci U S A*. 2010;107:12564–12569.

64. McCloy RA, Rogers S, Caldon CE, Lorca T, Castro A, Burgess A. Partial inhibition of Cdk1 in G 2 phase overrides the SAC and decouples mitotic events. *Cell Cycle*. 2014;13:1400–1412.

Investigative Ophthalmology & Visual Science